A Phenomenological study on the wino radiative decay in anomalous $U(1)'$ models

Francesco Fucito[a], Andrea Lionetto[a], Antonio Racioppi[b], Daniel Ricci Pacifici[a]

[a]*Dipartimento di Fisica dell'Università di Roma ,"Tor Vergata" and I.N.F.N. - Sezione di Roma "Tor Vergata",*
Via della Ricerca Scientifica, 1 - 00133 Roma, ITALY
[b]*National Institute of Chemical Physics and Biophysics, Ravala 10, Tallinn 10143, Estonia*

Abstract

An extension of the Standard Model by at least one extra U(1) gauge symmetry has been investigated by many authors. In this paper we explore the possibility that this extra U(1) is anomalous. One of the possible signatures of this model could be given by the photons produced in the decays of the NLSP into the LSP.

Keywords: Beyond the SM; LHC; Anomalous U(1) Models; NLSP Radiative Decay

1. Introduction

The start of the LHC has greatly motivated detailed phenomenological studies of scenarios which involve physics beyond the Standard Model (SM). Among them D-brane constructions in string theory are one of the most promising framework in which the SM can be embedded and extended. Such brane constructions naturally lead to extra anomalous $U(1)$'s in the four dimensional low energy theory and, in turn, to the presence of possible heavy Z' particles in the spectrum. These particles should be among the early findings of LHC and besides for the above cited models they are also a prediction of many other theoretical models of the unification of forces (see [1] for a recent review). In [2] we have considered a minimal extension of the Minimal Supersymmetric Standard Model (MSSM) with a single extra $U(1)'$ gauge symmetry in a string-inspired setup. We believe that our model encodes the key features of the low-energy sector of some of those brane construction. In this framework we studied in [3] the radiative decay of the next to lightest supersymmetric particle (NLSP) into the lightest supersymmetric particle (LSP). This kind of process is very interesting since it might be the first one where the LSP could be observed at LHC [4, 5] and at the upcoming ILC [6, 7].

2. Preliminaries and Lagrangian

Under suitable assumptions the LSP in our model turns out to be an axino [8], the fermion component of the Stückelberg supermultiplet related to the anomaly cancellation mechanism (see for details [2, 3, 8]). Without loss of generality we assume a wino-like NLSP. In the following we just give the interaction term which involve the axino and the wino relevant for our analysis. The interaction term, written in terms of four components Majorana spinors[1], is given by

$$ i\mathrm{L} = \sqrt{2}\sin\theta_W \frac{g_0 \mathcal{A}^{(2)}}{M_{Z'}} \frac{g_2^2}{32\pi^2} \bar{\lambda}_2 \gamma_5 [\gamma^\mu, \gamma^\nu](\partial_\mu A_\nu)\psi_S \qquad (1) $$

where λ_2 is the neutral wino, ψ_S is the axino, A_ν is the photon, θ_W the Weinberg angle, g_0 and g_2 respectively the $U(1)'$ and $SU(2)$ coupling constants, $\mathcal{A}^{(2)}$ the $U(1)'-SU(2)-SU(2)$ anomaly factor and $M_{Z'}$ the Z' mass. The rate of the radiative decay ($\lambda_2 \to \Psi_S \gamma$) is

$$ \Gamma_\gamma^{(2)} = g_2^4 \sin^2\theta_W \left(\frac{g_0 \mathcal{A}^{(2)}}{M_{Z'}}\right)^2 \frac{(\Delta M)^3(\Delta M + 2M_S)^3}{1024\pi^5(\Delta M + M_S)^3} \quad (2) $$

where $\Delta M = M_2 - M_S$, while M_2 and M_S are respectively the wino and axino masses. As we showed in [3], the radiative decay is the most dominant wino decay mode with a BR close to 1 ($\gtrsim 94\%$), so we can use (2) to give an estimation of the wino mean life time

$$ \tau_{\lambda_2} \simeq \frac{\hbar}{\Gamma_\gamma^{(2)}} \qquad (3) $$

3. LHC Phenomenology

In order to fall into the WMAP range in the most experimentally attractive situation, we considered a light LSP ($115\,\mathrm{GeV} \lesssim M_S \lesssim 150\,\mathrm{GeV}$) and a mass gap of order $\Delta M/M_S \simeq 20\%$, which imply more energetic and therefore easier to detect photons. This requirement is necessary because the detector resolution increases with energy, while at low energy there is an obstruction for the detection of photons due to bremsstrahlung, QCD background and absorption before the detection from the calorimeter [9].

Moreover we considered a universal squark mass $M_{\tilde{Q}}$ for

---

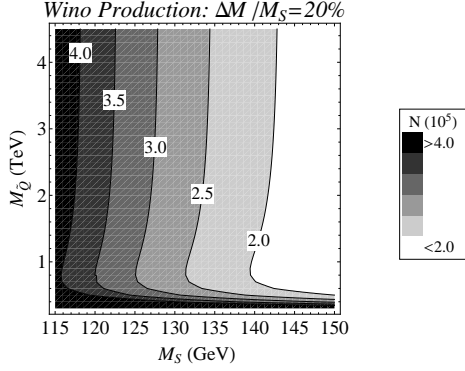[1]The gamma matrices γ^μ are in the Weyl representation.

Figure 1: Number of directly produced winos in function of the axino mass M_S and the universal squark mass $M_{\tilde{Q}}$.

the first two squark generations (since under this assumption they are nearly degenerate) and we assumed flavor blindness [10]. The contribution from the third generation squarks is always negligible. In Fig. 1 we summarize the results obtained in [3] by plotting the number of directly produced winos as a function of M_S and $M_{\tilde{Q}}$ having assumed 14 TeV of center of mass energy and 100 fb^{-1} of integrated luminosity. Since the BR is almost close to one this is also the number of photons in the final state. The number of photons produced is of the order of 10^5. In our analysis we follow [9],[11]-[13], where the NLSP decay in the GMSB framework is controlled by the parameter C_{grav}. If the NLSP lifetime is not too long ($C_{grav} \sim 1$) photons originate close to the primary interaction vertex ("prompt photons"). In the case of large C_{grav} and therefore long lived neutralinos the resulting photons are non-pointing. From now on we fix the axino mass $M_S \simeq 124$ GeV and the universal squark mass $M_{\tilde{Q}} \simeq 3.5$ TeV. In our framework the role of C_{grav} is played by the ratio $g_0\mathcal{A}^{(2)}/M_{Z'}$. In the following we discuss two different cases: short lived NLSP and long lived one.

3.1. Short life time

We compare the number of photons produced by radiative decay with the ones produced by the cascade decays of all the other supersymmetric processes. We slightly modified the Herwig code 6.5 [14] in order to take into account the new axino state in the neutral sector. It should be stressed that Herwig does not implement extra Z' in a supersymmetric framework. This in turn implies that the total number of photons can be underestimated due to the lack of sparticles interactions with the Z'. However this problem can be overcome by assuming a decoupled Z' either because it is very heavy or because it is extra-weak coupled. We generated by Herwig 2-partons$\rightarrow$ 2-sparticles events, using about 1 fb^{-1} of integrated luminosity but we have not considered the case of SM particles produced directly in the parton-parton
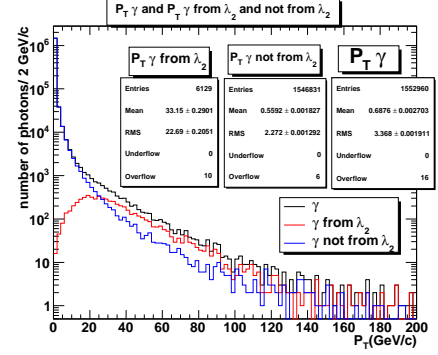

Figure 2: P_T distribution of photons (in log scale) for 10^4 susy events.
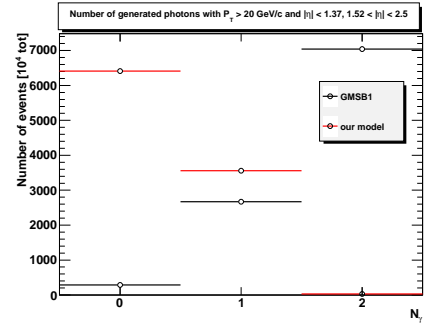

Figure 3: Number of generated photons before the preselection cuts.

interaction. A good discriminant variable of the process is the P_T of the photons produced by radiative decay, in particular in the region of P_T between 30-80 GeV/c. The corresponding distribution is shown in Fig. 2. We denote in red the number of γ's radiatively produced from the decay of the wino, in blue the number of γ's from all the other processes while in black the sum of the two. We assumed $\tau_{\lambda_2} \simeq 1.29 \cdot 10^{-15}s$, which is obtainable with $M_{Z'} \simeq 1$ TeV and $g_0\mathcal{A}^{(2)} \simeq 0.2$. We performed the same cut on the number of generated photons as in [13] with $P_T > 20$ GeV and with pseudorapidity $|\eta| \leq 1.37$, $1.52 < |\eta| < 2.5$, which provides a good way to further suppress the SUSY background[2]. The result obtained by using Herwig in generating 10^4 net events is given in Fig. 3. The most important difference between our case and the GMSB1 sample [9, 11, 12] is in the number of events with zero or two photons in the final state. The latter in particular is only 30 in our case. This behavior can be related to the squark masses we have considered. In our case they are about 3.5 TeV, while in the GMSB1 they are lower than 1 TeV ($\sim$ 900 GeV). We choose the value of 3.5 TeV for the squark masses since in this case the number of directly produced winos essentially depends only on M_S (see Fig. 1). The number of produced squarks is low since they have a high mass.

---

[2]After having employed the SUSY preselection cut which we describe later.

Hence they give a lower contribution to the NLSP production. If we consider lighter squarks, with masses less than 1 TeV, there is an increasing in the number of events with 2 photons in the final state. In any case the channel with one photon in the final state is always the dominant one.

The key point in the analysis is the SM background discrimination. We considered the same SM background as in [13]: events with QCD jets, single gauge bosons (W and Z) production, di-Boson, $\gamma\gamma$ and $t\bar{t}$ production. In order to disentangle the SM background from the signal we require a standard preselection cut for SUSY-like signatures:

- at least four jets must be present with $p_T > 50$ GeV ($p_T > 100$ GeV for the leading jet);

- missing transverse energy $E_T^{miss} > 60$ GeV.

After having applied these preselection cut we are able to reconstruct photons with $p_T > 20$ GeV and $|\eta| \leq 1.37$, $1.52 < |\eta| < 2.5$. The jet-finder algorithm used in our analysis is the Durham-type clustering KTCLUS [15]. The cut on the E_T^{miss} requires some care. In hadron colliders, the initial momentum of the colliding partons along the beam axis is not known since the energy of each hadron is distributed and constantly exchanged between the partons. Hence the total amount of missing energy cannot be determined in a straightforward way. However the initial energy of particles travelling transverse to the beam axis is zero and thus any net momentum in the transverse direction denotes missing transverse energy. To determine the latter for the i-th not-detected particle in each generated event, we considered the following procedure: take a transverse direction (perpendicular to the z axis) and define the vector

$$(\overrightarrow{E}_T^{miss})_i = E_i \left(\frac{\overrightarrow{P}_T}{|\overrightarrow{P}|} \right)_i$$

whose direction is given by its momentum. Then $E_T^{miss} = \sqrt{[(E_T^{miss})_x^{TOT}]^2 + [(E_T^{miss})_y^{TOT}]^2}$ where $(\overrightarrow{E}_T^{miss})_x^{TOT} = \sum_i ((\overrightarrow{E}_T^{miss})_x)_i$ and analogously for the y component. The result is shown in Fig. 4. In this plot the number of photons from the NLSP decay is that generated by Herwig while the number of background photons is the reconstructed one [13]. We note that in the channels with $N_\gamma \geq 1$ the signal can be easily disentangled by the SM background.

3.2. Long life time

In the case in which the wino is a long lived particle the reconstruction of the emitted photon after its decaying plays an important role. If the NLSP has a significant decay length, a photon will not "point back" to the primary interaction point (O in Fig. 5) but towards a kind
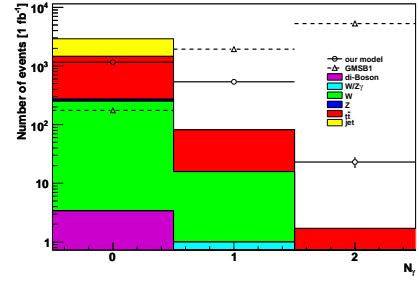

Figure 4: Number of generated photons per event for our model and for GMSB1 and number of reconstructed photons for the SM background, after having applied the cuts described in the main text.
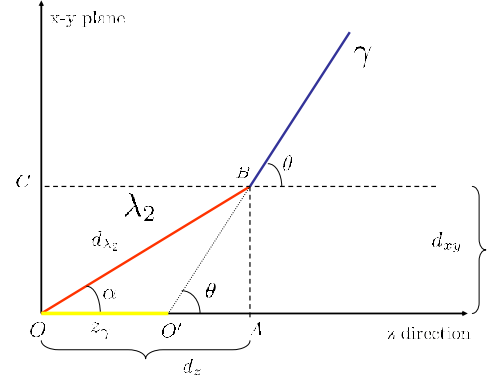

Figure 5: Schematic diagram of a non-pointing photon. d_{λ_2} is the distance traveled by λ_2 before its radiative decay. z_γ is the value of the displaced vertex.

of "virtual" point (O'). The relevant discriminant variable is z_γ, the distance between O and O'. Using simple trigonometric relations we have:

$$z_\gamma = d_z - d_{xy} \cot \theta \qquad (4)$$

with $\cot \theta = P_Z^\gamma / P_T^\gamma$, the ratio between the photon momentum along the beam direction (z-axis) and the transverse momentum.

By fitting the vertex resolution along z as a function of the photon energy for $|\eta| < 0.5$ (see plot in section "Electrons and Photons" in [9]) we derive the functional dependence of the standard deviation σ for the Gaussian distribution associated to z_γ on the energy in GeV of all the photons as

$$\frac{\sigma}{\text{mm}} \simeq 0.7\sqrt{E/\text{GeV}} + \frac{65}{\sqrt{E/\text{GeV}}} \qquad (5)$$

To each z_γ we can associate a random number sampled from a Gaussian distribution centered on that specific value of z_γ and with σ given by the relation in (5). We considered a wino mean life time $\tau_{\lambda_2} \sim 3.463 \cdot 10^{-10}$ s, so that the distance travelled by this particle before its radiative decay is always within the ATLAS tracker radius (~ 115 cm). In Fig. 6 we show the results of the analysis
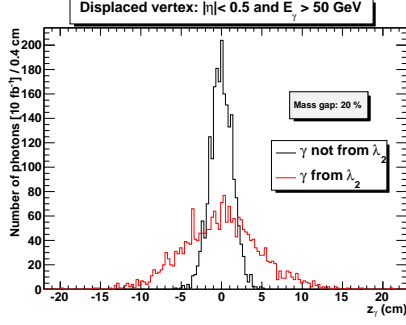
3

Figure 6: Displaced vertex z_γ for photons of $E > 50$ GeV and $|\eta| < 0.5$: the red line stands for photons produced by wino decay, the black one for photons from the other susy processes.

for photons of $E > 50$ GeV and with $|\eta| < 0.5$ (photons with great angle to the beam direction, because these are more easily detected than the ones along the z direction), for an integrated luminosity of $10~fb^{-1}$. By considering the value of their energy and the contribution of the tail of the associated Gaussian distribution, we observe a consequent enlargement of the distribution of γ's not coming from λ_2, which otherwise would be a spike centered on the origin of the x-axis in Fig. 6. The red line stands for photons produced by radiative wino decay, while the black one from the others SUSY processes. We can see that in the region $|z_\gamma| > 3$ cm the photons from the radiative decay are well distinguished from the background ones. Since we have assumed $\Delta M/M_S = 20\%$, $M_S \simeq 124$ GeV and $\tau_{\lambda_2} \sim 3.463 \cdot 10^{-10}$ s, we get from (3)

$$\frac{g_0 \mathcal{A}^{(2)}}{M_{Z'}} \simeq \frac{3.9 \cdot 10^{-4}}{\text{TeV}} \qquad (6)$$

To satisfy (6) we need either a super-heavy Z' ($M_{Z'} \simeq 385$ TeV if $g_0 \mathcal{A}^{(2)} \simeq 0.15$) or an extra-weakly coupled ($g_0 \mathcal{A}^{(2)} \simeq 0.00039$ if $M_{Z'} \simeq 1$ TeV) one. This decoupling makes our simulation more consistent since in it we have neglected the Z' contribution. Cases of extra-weak Z' were already studied in the past [1, 16].

4. Conclusion

The most important result we get is shown in Fig. 6 which gives a distinctive behavior of the photons coming from our model with respect to those coming from other SUSY processes. The distribution of z_γ is centered in zero while the half-width is a function of the NLSP decay length d_{λ_2}. This means that the radiative produced photons are preferably emitted along the NLSP direction or more generally at very small angle. Thus the signal can be disentangled from the background by applying a suitable cut in a region $|z_\gamma| \lesssim 5$ cm. Our result can be compared with [9] in which the NLSP is a long lived wino-like particle in the particular gauge mediated model dubbed GMSB3. The main difference is in the mass gap. In our model we considered a mass gap of 20% and an

LSP of 124 GeV, while in the GMSB3 case the mass gap is much higher: the gravitino (the LSP) is almost massless ($m_{\tilde{G}} = 1.08 \cdot 10^{-8}$ GeV) and the NLSP has a mass $m_{\tilde{\chi}_1} = 118.8$ GeV. In this case the energy distribution for the photons produced by the NLSP decay is peaked on the value of the NLSP mass $E \simeq m_{\tilde{\chi}_1} = 118.8$ GeV while in our case the peak is around 20 GeV. Moreover in the GMSB3 $c\tau_{\tilde{\chi}_1} \simeq 3.2$ m and so the NLSP long lived particles tend to escape the detector before their decay. This implies a sizable reduction in the number of photons detected.

References

[1] P. Langacker, arXiv:0801.1345 [hep-ph].

[2] P. Anastasopoulos, F. Fucito, A. Lionetto, G. Pradisi, A. Racioppi and Y. S. Stanev, Phys. Rev. D **78** (2008) 085014 [arXiv:0804.1156 [hep-th]].

[3] A. Lionetto and A. Racioppi, Nucl. Phys. B **831** (2010) 329 [arXiv:0905.4607 [hep-ph]].

[4] H. Baer and T. Krupovnickas, JHEP **0209** (2002) 038 [arXiv:hep-ph/0208277].

[5] H. Baer, A. Mustafayev, E. K. Park and X. Tata, JHEP **0805** (2008) 058 [arXiv:0802.3384 [hep-ph]].

[6] H. K. Dreiner, O. Kittel and U. Langenfeld, Phys. Rev. D **74** (2006) 115010 [arXiv:hep-ph/0610020].

[7] R. Basu, P. N. Pandita and C. Sharma, Phys. Rev. D **77** (2008) 115009 [arXiv:0711.2121 [hep-ph]].

[8] F. Fucito, A. Lionetto, A. Mammarella and A. Racioppi, arXiv:0811.1953 [hep-ph].

[9] G. Aad *et al.* [The ATLAS Collaboration], arXiv:0901.0512 [hep-ex].

[10] H. Baer and X. Tata, "Weak scale supersymmetry: From superfields to scattering events," *Cambridge, UK: Univ. Pr. (2006) 537 p*

[11] D. Prieur, arXiv:hep-ph/0507083.

[12] M. Terwort [ATLAS Collaboration and CMS Collaboration], arXiv:0805.2524 [hep-ex].

[13] M. Terwort, "Study of GMSB models with photon final states using the ATLAS detector", PhD DESY-THESIS, 2009. http://www-atlas.desy.de/theses.html

[14] G. Corcella *et al.*, JHEP **0101** (2001) 010 [arXiv:hep-ph/0011363].

[15] S. Catani, Y. L. Dokshitzer, M. H. Seymour and B. R. Webber, Nucl. Phys. B **406** (1993) 187.

[16] D. Feldman, Z. Liu and P. Nath, Phys. Rev. D **75** (2007) 115001 [arXiv:hep-ph/0702123].